



Patella radiograph image texture: The correlation with lumbar spine bone mineral density values

Agus Mulyono^{1*}, Md. Monirul Islam², Vishal R. Panse³

¹Department of Physics, State Islamic University of Maulana Malik Ibrahim Malang, Indonesia

²Department of Computer Science and Engineering, University of Information Technology & Sciences, Dhaka, Bangladesh

³Late. B. S. Arts, Prof. N. G. Science & A. G. Commerce College Sakharkherda, Sakharkherda, India

*Corresponding Address: gusmul@fis.uin-malang.ac.id

Article Info

Article history:

Received: January 31, 2022

Accepted: April 05, 2022

Published: April 29, 2022

Keywords:

BMD;
 Patella;
 Radiography;
 Texture image.

ABSTRACT

Osteoporosis is a common metabolic disease that is frequently overlooked. This disease primarily affects adult women and causes bone thinness and fragility, which leads to fractures. DXA (Dual Energy X-ray Absorptiometry) is used to diagnose osteoporosis by measuring bone mineral density. These devices are expensive and not widely available for treatment. This study aimed to find a correlation between the texture value of an image of the patellar bone and the density of the lumbar spine, which can then be used to detect osteoporosis. This study's sample size was 19 subjects, and their bone mineral density (BMD) was measured using DXA. An X-ray was then taken to obtain an image of the genu bone. The stages of the research are as follows: 1) preparing the X-ray image of the bone; 2) determining the image texture value method of gray level co-occurrence matrix 3) investigating the relationship between texture values and BMD in the lumbar spine. The correlation test results revealed a statistically significant correlation between the texture value and the BMD of the lumbar spine for the correlation and variance characteristics (P less than 0.05). As a result, the value of the texture of the image of the patella bone can be used to detect osteoporosis.

© 2022 Physics Education Department, UIN Raden Intan Lampung, Indonesia.

INTRODUCTION

Osteoporosis is defined as a bone disease with low bone mass and microarchitectural damage to bone tissue (Liu et al., 2019), which leads to bone fragility and an increased risk of fracture (consensus), changes in bone architecture, and clinical consequences in the form of being prone to fracture (fractures) with minor or no trauma (Center, 2017). Fractures most commonly occur in bones with numerous trabeculae, such as the wrist (wrist), spine (spine), and groin (femur) (Adams, 2013).

Disability as a result of hip, spine, or wrist fractures can reduce a patient's quality of life while also increasing the financial burden on the healthcare system (Mithal et al., 2014). Furthermore, the risk of death following osteoporosis-related fractures rises

(Cauley, 2013). Osteoporosis develops as bone density declines with age (Sozen et al., 2017). When you're young, your bones grow and heal on their own. Bones stop growing at 16-18 years old, but bone mass continues to increase until the late 20s. This process, however, will be accompanied by the passage of time. As people age, their density decreases. Bones become weaker, porous, and more prone to fracture (Zioupou et al., 2020).

Measuring bone mineral density (BMD) in high-risk groups is an important step toward lowering the prevalence of osteoporosis. The world health organization (WHO) uses Dual Energy X-Ray Absorptiometry (DEXA) as the gold standard for BMD examination (Diamond & Sheu, 2016). Despite the error correction on

DEXA, it is the standard technique for measuring bone density (Link & Kazakia, 2020) (Martineau et al., 2021). BMD and T-score values that reflect bone density based on the mineral content in bone are the results of measuring bone mass density using the DEXA technique (Ralston & Fraser, 2015). DEXA cannot distinguish between the cortex and the trabecular (D'Elia et al., 2009). As a result, in addition to bone mass density, we require a method that can reflect bone microarchitecture as an indicator of bone quality (Yong & Logan, 2021).

Radiographically, the texture feature is one of the most important factors in determining bone architecture, including the patella bone in the knee. The gray level co-occurrence matrix (GLCM) method is one for extracting texture information from an image (Pratiwi et al., 2015; Gebejes et al., 2013). As a result, it is critical to understand the relationship between texture characteristics and BMD values in the lumbar spine.

Many studies on bone image texture analysis have been conducted. Texture analysis on jawbone images to detect osteoporosis (Sela, 2021), hand bones (Insania et al., 2018), and hip bone texture analysis (Hirvasniemi et al., 2019). However, no one has ever used an image of the patella bone to analyze its texture. As a result, the image of the patella bone will be used as the object of analysis in this study.

METHODS

A radiograph of the patellar bone and the results of the lumbar spine density examination were used in this study. The radiograph image's texture is then examined using the gray level co-occurrence matrix method. The following are the research steps.

The first step is to collect data from the study sample on osteoporosis and normal status. These measurements were obtained using a densitometry (DXA) tool. An x-ray of the knee bone was then taken from the sample to obtain an image of the knee/genu.

The second step is to use Matlab to determine the texture value of the patella using the gray level co-occurrence matrix method. The third step is to examine the relationship between the texture value of the patella image and the lumbar spine BMD value (Fig.1). BMD values are obtained from DXA measurements.

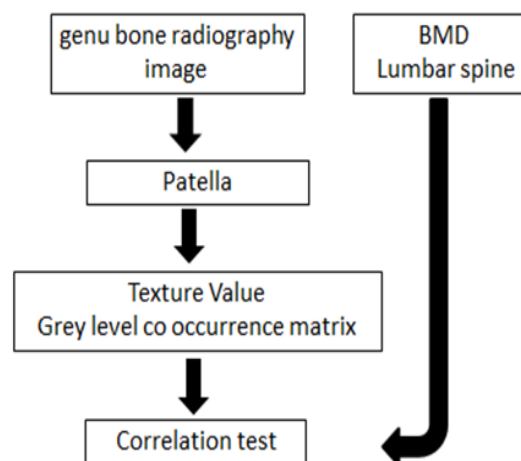


Figure 1. Research Flow

RESULTS AND DISCUSSION

From 19 people measured by Densitometry (DXA), a tool for detecting osteoporosis standard WHO, the researchers obtained the following data: example of the examination of the lumbar spine BMD (fig.2).

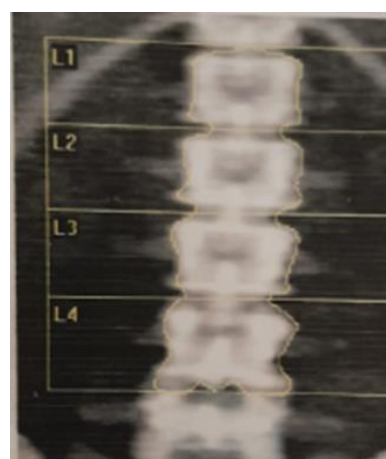


Figure 2. Lumbar Spine BMD Examination

In the lumbar spine BMD examination, BMD values were obtained in section L1, section L2, section L3, and section L4. The

BMD examination results data are displayed in table 1.

Table 1. Lumbar Spine BMD Values

No	BMD L1	BMD L2	BMD L3	BMD L4
1	0.806	0.929	1.025	1.03
2	0.569	0.575	0.587	0.585
3	0.61	0.704	0.691	0.799
4	0.373	0.449	0.499	0.584
5	0.614	0.681	0.679	0.74
6	0.333	0.394	0.487	0.552
7	0.728	0.862	0.905	0.875
8	0.511	0.605	0.639	0.673
9	0.423	0.514	0.652	0.647
10	0.683	0.817	0.899	0.955
11	0.891	0.931	1.022	1.088
12	0.934	1.09	1,207	1.172
13	0.567	0.657	0.74	0.777
14	0.567	0.638	0.673	0.735
15	0.462	0.523	0.488	0.495
16	0.856	0.934	0.899	1.151
17	0.796	0.846	0.835	0.963
18	0.913	0.982	0.924	1.157
19	0.789	0.876	0.865	1.04

Figure 3 displays the sample image results of bone genu radiography with the specifications of the SHIMADZU MODEL XUD 150L-30F. 150 kv 500mA.



Figure 3. Radiograph Image of Bone Genu

The gray level co-occurrence matrix method extracted texture features from radiographic images of the genu bone and patellar trabeculae. Table 2 displays the results of the texture analysis of the patellar trabeculae.

Table 2. Sample Texture Values of the Patella bone Using the Gray Level Co-Occurance Matrix Method

Texture Features	Value
Angular Second Moment	0.001 0.001 0.001 0.001 0.001 etc.
Contrast	100.22 67.581 104.41 150.57 88.039 etc.
Correlation	0.951 0.723 0.722 0.786 0.767 etc.
Variance	976.16 88.213 135.33 276.73 144.95 etc.
Inverse Different Moment	0.152 0.149 0.124 0.102 0.134 etc.
Entropy	11,491 10,267 10,696 11,387 10,697 etc.

The texture value of the patellar bone image was then correlated with the BMD value of the lumbar spine in sections L1, L2, L3, and L4. Table 3 displays the correlation test results.

Table 3 shows that the texture value at the angular second moment does not correlate with BMD L1, L2, L3, and L4 ($P > 0.05$). The contrast value is also unrelated to BMD L1, L2, L3, and L4 ($P > 0.05$). The Correlation value was correlated with the BMD L1, L2, L3, and L4 values ($P < 0.05$). The variance value was also correlated with the BMD L1, L2, L3, and L4 values ($P < 0.05$). The inverse different moment value does not correlate with BMD L1, BMD L2, BMD L3, or BMD L4 values ($P > 0.05$), and entropy does not correlate with BMD L1, BMD L2, BMD L3, or BMD L4 values ($P > 0.05$).

Table 3. The Results of the Pearson Correlation Test Between Texture Values and BMD of the Lumbar Spine

Texture Value/ BMD	BMD L1	BMD L2	BMD L3	BMD L4
Angular Second Moment	r = - 0.421 sig = 0.072	r = - 0.346 sig = 0.147	r = - 0.198 sig = 0.416	r = - 0.393 sig = 0.096
Contrast	r = 0.091 sig = 0.712	r = 0.051 sig = 0.836	r = 0.025 sig = 0.920	r = 0.143 sig = 0.560
Correlation	r = 0.478 sig = 0.039	r = 0.495 sig = 0.031	r = 0.500 sig = 0.029	r = 0.550 sig = 0.015
Variance	r = 0.604 sig = 0.006	r = 0.586 sig = 0.008	r = 0.552 sig = 0.014	r = 0.635 sig = 0.003
Inverse Different Moment	r = 0.287 sig = 0.234	r = 0.321 sig = 0.181	r = 0.341 sig = 0.153	r = 0.255 sig = 0.291
Entropy	r = 0.298 sig = 0.215	r = 0.293 sig = 0.224	r = 0.286 sig = 0.236	r = 0.380 sig = 0.109

The correlation value was moderately correlated with the lumbar spine BMD value, and the variance value was strongly correlated with the lumbar spine BMD value.

The number of trabeculae in postmenopausal osteoporosis patients will decrease due to a decrease in estrogen, which regulates the formation of collagen, non-collagenous protein matrix, and mineralization (Zhibin et al., 2015). Reducing estrogen by up to 75% has been shown to stimulate pro-inflammatory cytokines in synovial fluid and internal condyles (Garza et al., 2019). Because the trabeculae have a high metabolism, this process can occur up to 5-8 times more frequently than in the cortical portion (White, 2014). Changes on the surface of the trabeculae that result in trabecular thinning, plate-type trabecular perforation, reduced trabecular branching, and marrow area expansion can lead to osteoporosis if they continue (Yang et al., 2003). This condition alters the X-ray absorption conditions in the bone, resulting in variations in the grayscale contrast recorded in the image.

Feature extraction is a critical component of recognizing the osteoporosis system. The GLCM method can be used to determine whether or not images have an

osteoporosis (Deoker & Pat, 2017). A combination of GLCM and RLM can be used to detect bone loss (Yousfi et al., 2019). The GLCM, SVM, and dental panoramic are also useful for detecting normal bone and osteoporosis (Hwang et al., 2017, Valentinitsch et al., 2019).

Texture analysis of the jawbone for osteoporosis detection using GLCM was successfully applied to Korean women (Kavitha et al., 2012). Also, texture analysis with GLCM is good for measuring bone quality (Shirvaikar et al., 2016). Furthermore, texture analysis on head CT images was used to distinguish normal bone density (Kawashima et al., 2019). Lastly, texture analysis with GLCM combined with artificial neural network methods on hand bones is also quite good for detecting osteoporosis (Su et al., 2020).

The image GLCM feature extraction shows indications to separate between normal and osteoporosis classes, best with feature extraction for distance = 1 and the observed angle orientations of 0°, 45°, 90°, and 135° (Azhari et al., 2014).

According to the findings of this study, the texture values obtained by the GLCM method can be used specifically to detect osteoporosis.

CONCLUSION

Texture correlation values were moderately strong and statistically significant ($p < 0.05$) correlated with BMD lumbar spine. Furthermore, the texture variance value was statistically significant ($p < 0.05$) and strongly correlated with the BMD value.

ACKNOWLEDGMENTS

The author would like to thank the State Islamic University of Maulana Malik Ibrahim Malang for the infrastructure to support this study.

AUTHOR CONTRIBUTIONS

All authors have contributions: Designed the study, performed the experiments, analyzed the data, wrote the manuscript,

REFERENCES

- Adams, J. E. (2013). *Dual-energy X-Ray. Osteoporosis and Bone Densitometry Measurements*. Medical Radiology. Springer, Berlin, Heidelberg. 101–122. https://doi.org/10.1007/174_2012_789
- Azhari, Suprijanto, Diputra, Y., Juliastuti, E., & Arifin, A. Z. (2014) Analisis citra radiografi panoramik pada tulang mandibula untuk deteksi dini osteoporosis dengan metode gray level cooccurrence matrix (GLCM) panoramic radiograph image analysis using cooccurrence gray level matrix method (GLCM) for early detection of O. *Mkb*, 46(1), 203–208.
- Cauley, J. A. (2013). Public health impact of osteoporosis. *Journals of Gerontology - Series A Biological Sciences and Medical Sciences*, 68(10), 1243–1251. <https://doi.org/10.1093/gerona/glt093>
- Center, J. R. (2017). Fracture burden: What two and a half decades of dubbo osteoporosis epidemiology study data reveal about clinical outcomes of osteoporosis. *Current Osteoporosis Reports*, 15(2), 88–95. <https://doi.org/10.1007/s11914-017-0352-5>
- D'Elia, G., Caracchini, G., Cavalli, L., & Innocenti, P. (2009). Bone fragility and imaging techniques. *Clinical Cases in Mineral and Bone Metabolism*, 6(3), 234–246.
- Deoker, M., & Pat, P. S. N. (2017). A review on osteoporosis detection by using CT images based on gray level co-occurrence matrix and rule based approach. *International Journal of Engineering Science and Computing*, 7(3), 4765–4767.
- Diamond, T., & Sheu, A. (2016). Bone mineral density: Testing for osteoporosis. *Australian Prescriber*, 39(2), 35–39.
- Garza, B. C. V., Cepeda, M. A. A. N., Hernandez, A. S., Martinez, M. G. O., Rangel, G. J., Romero, C. C., Delgadillo, R. H., & Soto, J. M. S. (2019). Idiopathic condylar resorption: Diagnosis, pathophysiology, treatment and orthodontic considerations. *International Journal of Applied Dental Sciences*, 87(3), 87–90.
- Gebejes, a, Master, E. M., & Samples, a. (2013). Texture characterization based on grey-level co-occurrence Matrix. *Conference of Informatics and Management Sciences*, 24(1) 375–378.
- Hirvasniemi, J., Gielis, W. P., Arbabi, S., Agricola, R., van Spil, W. E., Arbabi, V., & Weinans, H. (2019). Bone texture analysis for prediction of incident radiographic hip osteoarthritis using machine learning: Data from the Cohort Hip and Cohort Knee (CHECK) study. *Osteoarthritis and Cartilage*, 27(6), 906–914. <https://doi.org/10.1016/J.JOCA.2019.02.796>
- Hwang, J. J., Lee, J. H., Han, S. S., Kim, Y. H., Jeong, H. G., Choi, Y. J., & Park, W. (2017). Strut analysis for osteoporosis detection model using dental panoramic radiography. *Dentomaxillofacial Radiology*, 46(7) 1–10. <https://doi.org/10.1259/dmfr.20170006>
- Insania, W. H., Nurhasanaha, & Sampurnoa,

- J. (2018). Aplikasi geometri fraktal untuk identifikasi osteoporosis pada tulang tangan dengan metode analisis fourier 2D. *Prisma Fisika*, 6(1), 62–64.
- Kavitha, M. S., Asano, A., Taguchi, A., Kurita, T., & Sanada, M. (2012). Diagnosis of osteoporosis from dental panoramic radiographs using the support vector machine method in a computer-aided system. *BMC Medical Imaging*, 12, 1–11. <https://doi.org/10.1186/1471-2342-12-1>
- Kawashima, Y., Fujita, A., Buch, K., Li, B., Qureshi, M. M., Chapman, M. N., & Sakai, O. (2019). Using texture analysis of head CT images to differentiate osteoporosis from normal bone density. *European Journal of Radiology*, 116, 212–218. <https://doi.org/10.1016/j.ejrad.2019.05.009>
- Link, T. M., & Kazakia, G. (2020). Update on Imaging-Based Measurement of Bone Mineral Density and Quality. *Current Rheumatology Reports*, 22(5), 1–11. <https://doi.org/10.1007/s11926-020-00892-w>
- Liu, P., Liang, X., Li, Z., Zhu, X., Zhang, Z., & Cai, L. (2019). Decoupled effects of bone mass, microarchitecture and tissue property on the mechanical deterioration of osteoporotic bones. *Composites Part B: Engineering*, 177(August), 107436. <https://doi.org/10.1016/j.compositesb.2019.107436>
- Martineau, P., Morgan, S. L., & Leslie, W. D. (2021). Bone mineral densitometry reporting: Pearls and pitfalls. *Canadian Association of Radiologists Journal*, 72(3), 490–504. <https://doi.org/10.1177/0846537120919627>
- Mithal, A., Bansal, B., Kyer, S. C., & Ebeling, P. (2014). The Asia-Pacific Regional audit-epidemiology, costs, and burden of osteoporosis in india 2013: A report of International Osteoporosis Foundation. *Indian Journal of Endocrinology and Metabolism*, 18(4), 449–454. <https://doi.org/10.4103/2230-8210.137485>
- Pratiwi, M., Alexander, Harefa, J., & Nanda, S. (2015). Mammograms classification using gray-level co-occurrence matrix and radial basis function neural network. *Procedia Computer Science*, 59(Iccsci), 83–91. <https://doi.org/10.1016/j.procs.2015.07.340>
- Ralston, S. H., & Fraser, J. (2015). Diagnosis and management of osteoporosis. *The Practitioner*, 259(1788), 15–19, 2. <https://europepmc.org/article/med/26882774>
- Sela, E. I. (2021). Deteksi osteoporosis pada citra radiograf panoramik dental menggunakan algoritme J48 dan learning vector quantization. *Jurnal Teknologi Dan Sistem Komputer*, 9(4), 211–217. <https://doi.org/10.14710/JTSISKOM.2021.14197>
- Shirvaikar, M., Huang, N., & Dong, X. N. (2016). The measurement of bone quality using gray level co-occurrence matrix textural features. *Journal of Medical Imaging and Health Informatics*, 6(6), 1357–1362. <https://doi.org/10.1166/JMIHI.2016.1812>
- Sozen, T., Ozisik, L., & Calik Basaran, N. (2017). An overview and management of osteoporosis. *European Journal of Rheumatology*, 4(1), 46–56. <https://doi.org/10.5152/eurjrheum.2016.048>
- Su, R., Liu, T., Sun, C., Jin, Q., Jennane, R., & Wei, L. (2020). Fusing convolutional neural network features with hand-crafted features for osteoporosis diagnoses. *Neurocomputing*, 385, 300–309. <https://doi.org/10.1016/j.neucom.2019.12.083>
- Valentinitsch, A., Trebeschi, S., Kaesmacher, J., Lorenz, C., Löffler, M. T., Zimmer, C., Baum, T., & Kirschke, J. S. (2019). Opportunistic osteoporosis screening in

- multi-detector CT images via local classification of textures. *Osteoporosis International*, 30(6), 1275–1285. <https://doi.org/10.1007/s00198-019-04910-1>
- White, S. C. (2014). Oral radiographic predictors of osteoporosis. *Dentomaxillofac Radiol*, 31(2), 84–92. <https://doi.org/10.1038/SJ.DMFR.4600674>
- Yang, J., Pham, S. M., & Crabbe, D. L. (2003). Effects of oestrogen deficiency on rat mandibular and tibial microarchitecture. *Dentomaxillofacial Radiology*, 32(4), 247–251. <https://doi.org/10.1259/DMFR/12560890>
- Yong, E. L., & Logan, S. (2021). Menopausal osteoporosis: Screening, prevention and treatment. *Singapore Medical Journal*, 62(4), 159–166. <https://doi.org/10.11622/SMEDJ.2021036>
- Yousfi, L., Houam, L., Boukrouche, A., Lespessailles, E., Ros, F., & Jennane, R. (2019). Texture analysis and genetic algorithms for osteoporosis diagnosis. *International Journal of Pattern Recognition and Artificial Intelligence*, 34(5), 1-20. <https://doi.org/10.1142/S0218001420570025>
- Zhibin, D., Steck, R., Doan, N., Woodruff, M. A., Ivanovski, S., & Xiao, Y. (2015). Estrogen deficiency associated bone loss in the maxilla: A methodology to quantify the changes in the maxillary intra-radicular alveolar bone in an ovariectomized rat osteoporosis model. *Tissue Eng Part C Methods*, 21(5) 458-66.
- Zioupos, P., Kirchner, H. O. K., & Peterlik, H. (2020). Ageing bone fractures: The case of a ductile to brittle transition that shifts with age. *Bone*, 131(1) 1-22. <https://doi.org/10.1016/j.bone.2019.115176>